Asociación Argentina
de Mecánica Computacional

Mecánica Computacional Vol XXIX, págs. 7967-7983 (artículo completo)
Eduardo Dvorkin, Marcela Goldschmit, Mario Storti (Eds.)
Buenos Aires, Argentina, 15-18 Noviembre 2010

FINITE ELEMENT DYNAMICAL SUB- GRID SCALE APPROXIMATION OF LOW MACH NUMBER FLOW EQUATIONS

M. Avila[a], J. Principe[a] and R. Codina[b]

[a]*International Center for Numerical Methods in Engineering (CIMNE), Technical University of Catalonia, Barcelona, Spain*

[b]*Department of Strength of Materials and Structural Engineering (RMEE), Technical University of Catalonia, Barcelona, Spain*

Keywords: Computational Fluid Dynamics, Low Mach, Variational Multiscale, Finite element analysis.

Abstract. In this work we propose a variational multiscale finite element approximation of thermally coupled low speed flows. The physical model is described by the low Mach number equations, which are obtained as a limit of the compressible Navier Stokes equations in the small Mach number. In contrast to the commonly used Boussinesq approximation, this model permits to take volumetric deformation into account. Although the former is more general than the later, both systems have similar mathematical structure and their numerical approximation can suffer the same type of instabilities.

We propose a stabilized finite element approximation based on the the variational multiscale method, in which a decomposition of the approximating space into a coarse scale resolvable part and a fine scale subgrid part is performed. Modeling the subscale and taking its effect on the coarse scale problem into account, results in a stable formulation. The quality of the final approximation (accuracy, efficiency) depends on the particular model.

The distinctive features of our approach are to consider the subscales as transient and to keep the scale splitting in all the nonlinear terms. The first ingredient permits to obtain an improved time discretization scheme (higher accuracy, better stability, no restrictions on the time step size). The second ingredient permits to prove global conservation properties. It also allows us to approach the problem of dealing with thermal turbulence from a strictly numerical point of view.

Numerical tests show that nonlinear and dynamic subscales give more accurate solutions than classical stabilized methods.

1 INTRODUCTION

The general description of a fluid flow involves the solution of the compressible Navier Stokes Equations. It is widely accepted that these equations provide an accurate description of any problem in fluid mechanics which may present many different nonlinear physical mechanisms. Depending on the physics of the problem under consideration, different simplified models describing some of these mechanisms can be derived from the compressible Navies Stokes equations.

Our application is directed to low speed strongly thermally coupled flows which are described by the compressible Navier Stokes equations in the low-Mach number limit. This limit is derived by an asymptotic expansion of the problem variables as power series of the small parameter $\gamma \mathrm{Ma}^2 << 1$, where γ denotes the specific heat ratio and Ma the Mach number of the problem. For details of this asymptotic expansion procedure, see (Principe and Codina, 2009; Majda and Sethian, 1985; Lions, 1996). As a particular result of this process, the total pressure is split into two parts, the thermodynamic part $p^{th}(t)$ which is uniform in space, and the hydrodynamic part $p(\boldsymbol{x},t)$ which is several orders of magnitude smaller than p^{th} and is neglected in the state and energy equations. This leads to a removal of the acoustic modes but large variations of density due to temperature variations are allowed. This system of equations is commonly used to describe problems of combustion in the form of deflagrations (i.e., flames at low speed).

Despite this important difference in the treatment of the incompressibility, the low Mach number equations present the same mathematical structure of the incompressible Navier Stokes equations (in the sense that the mechanical pressure is determined from the mass conservation constraint). Consequently the same type of numerical instabilities can be found, namely the problem of compatibility conditions between the velocity and pressure finite element spaces, and the instabilities due to convection dominated flows. These instabilities can be avoided by the use of stabilization techniques. Stabilized finite element methods (FEM) have been initially developed for the Stokes (Hughes et al., 1986) and for the convection diffusion reaction (CDR) problems (Codina, 1998). Later they have been extended to incompressible Navier Stokes equations (Codina, 2001; Hughes et al., 2004), and for the low Mach approximation (Principe and Codina, 2007) but the nonlinearity of the problem was not considered in their design. These extensions were essentially the application to nonlinear transient problems of a technique developed for linear steady ones.

The design of stabilization techniques considering the transient nonlinear nature of the problems began with the introduction of dynamic nonlinear subscales in (Codina, 2002; Codina et al., 2007). Developed in the context of the variational multiscale (VMS) concept introduced by Hughes (Hughes et al., 1998), the idea is to consider the subgrid scale time dependent and to consider its effect on all the non-linear terms, resulting in extra terms in the final discrete scheme. Important improvements in the discrete formulation of the incompressible Navier Stokes problem have been observed. From a theoretical point of view, the use of transient subgrid scales explains how the stabilization parameter should depend on the time step size and makes space and time discretizations commutative and the tracking of the subscales along the non-linear process provides global momentum conservation for incompressible flows. From a practical point of view, the use of time dependent non linear subscales results in a more robust and more accurate method (an unusual combination) as shown by numerical experiments (Codina, 2002; Codina et al., 2007).

These developments also opened the door to the use of numerical techniques to cope with

the potential instabilities and to model turbulence at the same time, as pointed out in (Codina, 2002; Codina et al., 2007). This is a natural step as turbulence is originated by the presence of the nonlinear convective term, as it is well known. The idea of modeling turbulence using only numerical ingredients actually goes back to (Boris et al., 1992) but it was fully developed for incompressible flows in (Bazilevs et al., 2007) and for low Mach number flows recently in (Gravemeier and Wall, 2010a) where quantitative comparisons against direct numerical simulations are presented. It is important to point out, however, that not all the terms arising from the nonlinear scale splitting are considered in these works. Apart from these results a careful analysis of the dissipative structure of the variational multiscale method with nonlinear time dependent subscales was presented in (Guasch and Codina, 2010; Principe et al., 2010), showing the physical interpretation of the method. This analysis was extended to thermally coupled flows using the Boussinesq approximation in (Codina et al., 2010).

In this article we consider the subgrid scale effect in **all** the non-linear terms in the low Mach number flow equations. We also consider the subgrid scales time dependent. It is shown that the method does not only provide the necessary stabilization of the formulation but also enables to obtain more accurate solutions than the classical linear approach for an equivalent mesh as happened for incompressible flows. It is also shown that global conservation properties for mass, momentum and energy are obtained from the final discrete scheme.

The paper is organized as follows. In section 2, the Low Mach number equations and its variational formulation is given. Afterwards the VMS formulation through dynamic scale splitting is derived in section 3. Time integration schemes are discussed in section 4. It is shown in section 5 that this formulation provides global mass, momentum and energy conservation when using equal interpolation spaces for the velocity, pressure and temperature equations. The formulation is tested for a stationary and a dynamic problem in section 6. Conclusions are drawn in section 7.

2 THE LOW MACH NUMBER EQUATIONS

2.1 Strong problem

Let $\Omega \subset \mathbb{R}^d$,with $d = 2, 3$, be the computational domain in which the flow takes place during the time interval $[0, T]$, and let $\partial\Omega$ be its boundary. The initial and boundary value problem to be considered consists in finding a velocity field $\boldsymbol{u}$, a hydrodynamic pressure field p, a temperature field T, and the thermodynamic pressure p^{th} such that

$$\frac{\partial \rho}{\partial t} + \boldsymbol{\nabla} \cdot (\rho \boldsymbol{u}) = 0 \quad \text{in } \Omega,\ t \in (0,T) \tag{1}$$

$$\rho \frac{\partial \boldsymbol{u}}{\partial t} + \rho \boldsymbol{u} \cdot \boldsymbol{\nabla} \boldsymbol{u} - \nabla \cdot (2\mu \boldsymbol{\varepsilon}'(\boldsymbol{u})) + \boldsymbol{\nabla} p = \rho \boldsymbol{g} \quad \text{in } \Omega,\ t \in (0,T) \tag{2}$$

$$\rho c_p \frac{\partial T}{\partial t} + \rho c_p \boldsymbol{u} \cdot \nabla T - \nabla \cdot k \nabla T - \alpha T \frac{dp^{th}}{dt} = Q \quad \text{in } \Omega,\ t \in (0,T) \tag{3}$$

where ρ denotes the density, μ the viscosity, $\varepsilon'(\boldsymbol{u}) = \varepsilon(\boldsymbol{u}) - \frac{1}{3}(\boldsymbol{\nabla} \cdot \boldsymbol{u})\boldsymbol{I}$ the deviatoric part of the rate of deformation tensor $\varepsilon(\boldsymbol{u}) = \boldsymbol{\nabla}^s \boldsymbol{u} = \frac{1}{2}\left(\boldsymbol{\nabla}\boldsymbol{u} + \boldsymbol{\nabla}\boldsymbol{u}^T\right)$, $\boldsymbol{I}$ the identity tensor, $\boldsymbol{g}$ the gravity force vector, c_p the specific heat coefficient at constant pressure, k the thermal conductivity, Q the heat source, and $\alpha = -\frac{1}{\rho}\frac{\partial \rho}{\partial T}|_p$ the thermal expansion coefficient. Equations (1)-(3) represent the mass, momentum and energy conservation respectively. Additionally the system must be closed by a state equation relating density ρ, thermodynamic pressure p^{th} and temperature T, of the form

$$\rho = \rho\left(T, p^{th}\right) \tag{4}$$

These equations must be supplied with initial and boundary conditions. Initial conditions are

$$\begin{aligned} \boldsymbol{u} &= \boldsymbol{u}_0 \ \text{ in } \Omega,\ t=0 \\ T &= T_0 \ \text{ in } \Omega,\ t=0 \\ p^{th} &= p_0^{th} \ \text{ in } \Omega,\ t=0 \end{aligned}$$

Dirichlet and Neumann boundary conditions for Eqs. (2) and (3) are

$$\begin{aligned} \boldsymbol{u} &= \boldsymbol{0} \ \text{ in } \Gamma_D^{\boldsymbol{u}} \\ T &= 0 \ \text{ in } \Gamma_D^{T} \\ (-p\boldsymbol{I} + 2\mu\boldsymbol{\varepsilon\prime}(\boldsymbol{u}))\cdot\boldsymbol{n} &= \boldsymbol{t}_n \ \text{ in } \Gamma_N^{\boldsymbol{u}} \\ k\boldsymbol{n}\cdot\boldsymbol{\nabla}T &= q_n \ \text{ in } \Gamma_N^{T}. \end{aligned}$$

where $\boldsymbol{n}$ is the outer unit normal on the boundary. It is assumed that $\Gamma_D^x \cup \Gamma_N^x = \partial\Omega$, and $\Gamma_D^x \cap \Gamma_N^x = \emptyset$ for $x = T, \boldsymbol{u}$.

Determination of thermodynamic pressure The time dependence of thermodynamic pressure $p^{th}(t)$ has to be determined independently of the Eqs. (1)-(3). For open flows $\left(\Gamma_N^{\boldsymbol{u}} \neq \emptyset\right)$ the thermodynamic pressure is given by the boundary conditions. For closed flows $\left(\Gamma_N^{\boldsymbol{u}} = \emptyset\right)$ the thermodynamic pressure is determined through global conservation equations over domain Ω, taking advantage of the uniformity of p^{th}.

In a closed system without inflow-outflow, the total mass remains constant over time, and p^{th} may be obtained each time subject to an integral form of the state equation

$$\int_\Omega \rho\left(T, p^{th}\right) \mathrm{d}\Omega = \int_\Omega \rho_0 \mathrm{d}\Omega \tag{5}$$

where $\rho_0 = \rho\left(T_0, p_0^{th}\right)$ is the initial density field.

In a closed system with inflow-outflow, the thermodynamic pressure may be determined by an equation obtained as a result of combining Eqs. (1), (3) and (4), given by

$$\frac{\alpha T}{\gamma - 1}\frac{dp^{th}}{dt} + \frac{\gamma}{\gamma - 1}\frac{\alpha T}{K}\nabla\cdot\boldsymbol{u} - \nabla\cdot(k\nabla T) = S \tag{6}$$

where γ, α and the compressibility coefficient $K = \frac{1}{\rho}\frac{\partial\rho}{\partial p}|_T$ is a thermodynamic function, depending on p^{th} and T. Integrating Eq. (6) over domain Ω yields an ordinary differential equation for p^{th} as

$$\frac{dp^{th}}{dt}\int_\Omega \frac{\alpha T}{\gamma - 1}\mathrm{d}\Omega + \int_\Omega \frac{\gamma}{\gamma - 1}\frac{\alpha T}{K}\nabla\cdot\boldsymbol{u}\mathrm{d}\Omega = \int_\Omega Q\mathrm{d}\Omega + \int_{\partial\Omega} \boldsymbol{n}\cdot k\nabla T\mathrm{d}\Gamma \tag{7}$$

subject to initial condition $p^{th}(t=0) = p_0^{th}$.

Ideal gases For ideal gases, the state equation is $\rho = p^{th}/RT$, with $R = \frac{\mathcal{R}}{M}$, where $\mathcal{R}$ is the universal gas constant and M the mean molecular mass. The thermal expansion and the compressibility coefficients for ideal gases are $\alpha = 1/T$ and $K = 1/p^{th}$respectively. Considering also uniform mean molecular mass (no combustion), Eqs. (5) and (7) take the form

$$p^{th} = p_0^{th}\frac{\int_\Omega \frac{1}{T_0}\mathrm{d}\Omega}{\int_\Omega \frac{1}{T}\mathrm{d}\Omega}$$

and

$$\frac{|\Omega|}{(\gamma-1)}\frac{dp^{th}}{dt}+\frac{\gamma}{\gamma-1}p^{th}\int_{\partial\Omega}\boldsymbol{n}\cdot\boldsymbol{u}\mathrm{d}\Gamma=\int_{\Omega}Q\mathrm{d}\Omega+\int_{\partial\Omega}\boldsymbol{n}\cdot k\nabla T\mathrm{d}\Gamma \tag{8}$$

respectively.

2.2 Variational formulation

To obtain a variational formulation for the system (1)-(3), let us denote by $\boldsymbol{V},Q,W$ the functional spaces where the solution is sought. When the Boussinesq approximation is considered they are given by $\boldsymbol{V}=\boldsymbol{L}^2\left(0,T;H^1\left(\Omega\right)^d\right)$, $Q=L^1\left(0,T:L^2\left(\Omega\right)\right)$, and $W=L^2\left(0,T;H^1\left(\Omega\right)\right)$ (Codina et al., 2010). For the low Mach number equations, the minimum regularity required is only known in very particular cases (Lions, 1996). The corresponding space of test functions will be denoted by $\boldsymbol{V}_0,Q_0,W_0$.

The weak form of the problem consists in finding $(\boldsymbol{u},p,T)\in(\boldsymbol{V},Q,W)$ such that

$$\left(\frac{\partial\rho}{\partial t},q\right)+\left(\nabla\cdot\left(\rho\boldsymbol{u}\right),q\right)=0\qquad\forall q\in Q^0\left(\Omega\right) \tag{9}$$

$$\begin{aligned}&\left(\rho\frac{\partial\boldsymbol{u}}{\partial t},\boldsymbol{v}\right)+\left(\rho\boldsymbol{u}\cdot\nabla\boldsymbol{u},\boldsymbol{v}\right)\\&+\left(2\mu\boldsymbol{\varepsilon}'\left(\boldsymbol{u}\right),\boldsymbol{\nabla}^s\boldsymbol{v}\right)-\left(p,\nabla\cdot\boldsymbol{v}\right)=\left(\rho\boldsymbol{g},\boldsymbol{v}\right)+\left(\boldsymbol{t}_n,\boldsymbol{v}\right)_{\Gamma_N^{\boldsymbol{u}}}\quad\forall\boldsymbol{v}\in\boldsymbol{V}_0\end{aligned} \tag{10}$$

$$\begin{aligned}&\left(\rho c_p\frac{\partial T}{\partial t},w\right)+\left(\rho c_p\boldsymbol{u}\cdot\nabla T,w\right)\\&+\left(k\nabla T,\nabla w\right)-\left(\alpha T\frac{dp^{th}}{dt},w\right)=\left(Q,w\right)+\left(q_n,w\right)_{\Gamma_N^T}\quad\forall w\in W_0\end{aligned} \tag{11}$$

where $(\cdot,\cdot)=(\cdot,\cdot)_\Omega$ and $(\cdot,\cdot)_\Gamma$ denote the L^2-inner product on Ω and Γ respectively.

3 SPACE DISCRETIZATION BY SCALE SPLITTING

Let us consider a finite element partition $\{K\}$ with n_e elements of the computational domain Ω, from which we can construct finite element spaces for the velocity, pressure and temperature in the usual manner. We will denote them by $\boldsymbol{V}_h\subset\boldsymbol{V}$, $Q_h\subset Q$ and $W_h\subset W$, respectively. We will assume that they are all built from continuous piecewise polynomials of the same degree k.

Let us split the continuous space $\boldsymbol{Y}=\boldsymbol{V}\times Q\times W$ as $\boldsymbol{Y}=\boldsymbol{Y}_h\oplus\widetilde{\boldsymbol{Y}}$, where $\widetilde{\boldsymbol{Y}}=\widetilde{\boldsymbol{V}}\times\widetilde{Q}\times\widetilde{W}$ is the subgrid space, that can be in principle any space to complete $\boldsymbol{Y}_h=\boldsymbol{V}_h\times Q_h\times W_h$ in $\boldsymbol{Y}$. The continuous unknowns split as

$$\boldsymbol{u}=\boldsymbol{u}_h+\widetilde{\boldsymbol{u}} \tag{12}$$

$$p=p_h+\widetilde{p} \tag{13}$$

$$T=T_h+\widetilde{T} \tag{14}$$

where the components with subscripts h belong to the corresponding finite element spaces, and the components with the $\widetilde{}$ correspond to the subgrid space. These additional components are what we will call subscales. Each particular variational multiscale method will depend on the way the subscales are approximated. We will consider these subscales time dependent and we will keep the previous decompositions (12)-(14) in all the terms of the variational problem (9) - (11). As we shall see, this has important consequences in the modeling of thermally coupled

turbulent flows. The only approximation we will make for the moment is to assume that the subscales vanish on the interelement boundaries, $\partial\Omega_e$. This happens for example if one assumes subscales as bubble functions, or that their Fourier modes correspond to high wave numbers, as it is explained in (Codina, 2002).

Substituting decompositions (12)-(14) in the variational problem (9) -(11), taking the tests functions in the corresponding finite element spaces and integrating some terms by parts, it is found that the solution $(\boldsymbol{u}_h, T_h, p_h) \in \boldsymbol{V}_h \times Q_h \times W_h$ must satisfy

$$\left(\frac{\partial \rho^h}{\partial t}, q_h\right) - \left(\rho^h \boldsymbol{u}_h, \nabla q_h\right) + \left(\rho^h \boldsymbol{n} \cdot \boldsymbol{u}_h q_h\right)_{\partial\Omega} - \left(\rho^h \widetilde{\boldsymbol{u}}, \nabla q_h\right) = 0 \tag{15}$$

$$\begin{aligned}
&\left(\rho^h \frac{\partial \boldsymbol{u}_h}{\partial t}, \boldsymbol{v}_h\right) + \left(\rho^h \left(\boldsymbol{u}_h + \widetilde{\boldsymbol{u}}\right) \cdot \nabla \boldsymbol{u}_h, \boldsymbol{v}_h\right) \\
&\quad + \left(2\mu \boldsymbol{\varepsilon}'\left(\boldsymbol{u}_h\right), \boldsymbol{\nabla}^s \boldsymbol{v}_h\right) - \left(p_h, \nabla \cdot \boldsymbol{v}_h\right) + \left(\rho^h \frac{\partial \widetilde{\boldsymbol{u}}}{\partial t}, \boldsymbol{v}_h\right) \\
&\quad - \left(\widetilde{\boldsymbol{u}}, - \frac{\boldsymbol{\partial} \rho^h}{\partial t} \boldsymbol{v}_h + \rho^h \left(\boldsymbol{u}_h + \widetilde{\boldsymbol{u}}\right) \cdot \boldsymbol{\nabla} \boldsymbol{v}_h - \boldsymbol{\nabla}^h \cdot \left(2\mu \boldsymbol{\varepsilon}\left(\boldsymbol{v}_h\right)\right)\right) \\
&\quad - \left(p', \nabla \cdot \boldsymbol{v}_h\right) = \left(\rho^h \boldsymbol{g}, \boldsymbol{v}_h\right) + \left(\boldsymbol{t}_n, \boldsymbol{v}_h\right)_{\Gamma_N^{\boldsymbol{u}}}
\end{aligned} \tag{16}$$

$$\begin{aligned}
&\left(\rho^h c_p \frac{\partial T_h}{\partial t}, w_h\right) + \left(\rho^h c_p \left(\boldsymbol{u}_h + \widetilde{\boldsymbol{u}}\right) \cdot \nabla T_h, w_h\right) \\
&+ \left(k \boldsymbol{\nabla} T_h, \nabla w_h\right) - \left(\alpha \frac{dp^{th}}{dt} T_h, w_h\right) + \left(\rho^h c_p \frac{\partial \widetilde{T}}{\partial t}, w_h\right) \\
&\quad - \left(\widetilde{T}, \alpha \frac{dp^{th}}{dt} w_h - c_p \frac{\boldsymbol{\partial} \rho^h}{\partial t} w_h + \rho^h \left(\boldsymbol{u}_h + \widetilde{\boldsymbol{u}}\right) \cdot \nabla w_h - \nabla^h \cdot \left(k \nabla w_h\right)\right) \\
&\quad = \left(Q, w_h\right) + \left(q_n, w_h\right)_{\Gamma_N^T}
\end{aligned} \tag{17}$$

for any tests function $(\boldsymbol{v}_h, q_h, w_h) \in (\boldsymbol{V}_{0,h}, Q_{0,h}, W_{0,h})$. The symbol ∇^h indicates that the integral is carried over the finite element interiors, and not over the edges, that is

$$\left(\widetilde{T}, \nabla^h \cdot \left(k \nabla w_h\right)\right) = \sum_K \left(\widetilde{T}, \nabla \cdot \left(k \nabla w_h\right)\right) \tag{18}$$

Applying the scale splitting to the state equation (4) we get the relation

$$\rho^h = \rho\left(T_h + \widetilde{T}, p^{th}\right) \tag{19}$$

used to give a closure to system (15) - (17). In the numerical examples it is shown that keeping the temperature subscale in the state equation improves the accuracy of the scheme. Notation ρ^h indicates that the obtained density for the discrete problem is different from density in the continuous problem. The use of a superscript instead of a subscript is because density does not belongs to any of the introduced finite element spaces.

Once the velocity subscale is approximated in the momentum equation (16), it provides additional terms than those that appear in classical stabilized finite element method, and some non standard terms in the sense that they are usually neglected. The terms involving the velocity subgrid scale arising from the convective term in the momentum equation $\left(\rho^h \widetilde{\boldsymbol{u}} \cdot \nabla \boldsymbol{u}_h, \boldsymbol{v}_h\right) -$

$\left(\widetilde{\boldsymbol{u}}, \rho^h \left(\boldsymbol{u}_h + \widetilde{\boldsymbol{u}}\right) \cdot \boldsymbol{\nabla} \boldsymbol{v}_h\right)$ can be understood as the contribution from the Reynolds- and cross-stress terms of a LES approach. Therefore, modeling $\widetilde{\boldsymbol{u}}$ implies modeling the subgrid scale tensor. The last row in (16) comes from the contribution of pressure subscale, that reinforces mass balance, and the contribution from the external forces. Similar comments to those made for the momentum equation apply to the energy equation (17). Once the temperature subscale is approximated it provides additional terms that appear in classical stabilized methods. The terms involving the velocity and temperature subgrid scale arising from the convective term $\left(\rho^h c_p \widetilde{\boldsymbol{u}} \cdot \nabla T_h, w_h\right) - \left(\widetilde{T}, \rho^h \left(\boldsymbol{u}_h + \widetilde{\boldsymbol{u}}\right) \cdot \nabla w_h\right)$ can be understood as the contribution from the Reynolds- and cross- stress terms of a LES approach, see (Codina et al., 2010). In the mass equation (15) the fourth term provides pressure stability once the velocity subscale is approximated.

To get the final numerical scheme we approximate the subscales in the element interiors. The finite element equations can be understood as the projection of the original equations onto the finite element spaces. The equations for the subscales are obtained by projecting onto their corresponding spaces $\widetilde{\boldsymbol{Y}}$. If $\widetilde{P}$ denotes the projection onto any of these spaces, the subscales equations are written as

$$\widetilde{P}\left(\rho^h \nabla \cdot \widetilde{\boldsymbol{u}} - \rho^h \alpha \left(\boldsymbol{u}_h + \widetilde{\boldsymbol{u}}\right) \cdot \nabla \widetilde{T}\right) = \widetilde{P}\left(R_c\right) \tag{20}$$

$$\widetilde{P}\left(\rho^h \frac{\partial \widetilde{\boldsymbol{u}}}{\partial t} + \rho^h \left(\boldsymbol{u}_h + \widetilde{\boldsymbol{u}}\right) \cdot \boldsymbol{\nabla} \widetilde{\boldsymbol{u}} - \nabla \cdot \left(2\mu \boldsymbol{\varepsilon}'\left(\widetilde{\boldsymbol{u}}\right)\right) + \nabla \widetilde{p}\right) = \widetilde{P}\left(\boldsymbol{R}_m\right) \tag{21}$$

$$\widetilde{P}\left(\rho^h c_p \frac{\partial \widetilde{T}}{\partial t} + \rho^h c_p \left(\boldsymbol{u}_h + \widetilde{\boldsymbol{u}}\right) \cdot \nabla \widetilde{T} - \nabla \cdot k \nabla \widetilde{T}\right) = \widetilde{P}\left(R_e\right) \tag{22}$$

where

$$R_c = -\frac{\partial \rho^h}{\partial t} - \rho^h \nabla \cdot \boldsymbol{u}_h + \rho^h \alpha \left(\boldsymbol{u}_h + \widetilde{\boldsymbol{u}}\right) \cdot \nabla T_h \tag{23}$$

$$\boldsymbol{R}_m = \rho^h \boldsymbol{g} - \rho^h \frac{\partial \boldsymbol{u}_h}{\partial t} - \rho^h \left(\boldsymbol{u}_h + \widetilde{\boldsymbol{u}}\right) \cdot \boldsymbol{\nabla} \boldsymbol{u}_h + \nabla \cdot \left(2\mu \boldsymbol{\varepsilon}'\left(\boldsymbol{u}_h\right)\right) - \nabla p_h \tag{24}$$

$$R_e = Q + \alpha \left(T_h + \widetilde{T}\right) \frac{dp^{th}}{dt} - \rho^h c_p \frac{\partial T_h}{\partial t} - \rho^h c_p \left(\boldsymbol{u}_h + \widetilde{\boldsymbol{u}}\right) \cdot \nabla T_h + \nabla \cdot \left(k \nabla T_h\right) \tag{25}$$

are the residuals of the finite element unknowns in the momentum, continuity and heat equation, respectively. Eqs. (20)-(22) need to be solved within each element Ω_e and completed with proper boundary conditions.

It is important to remark that modeling the gradients of the subscales is more involved than modeling the subscales themselves. Note that although all the unknowns are being split in Eqs. (15) - (17), those equations do not contain any subscale gradient nor any density gradient. This has been achieved by a proper by-parts integration of the continuous problem (9) - (11).

Approximation of the subscales Up to this point the only approximation introduced is to assume that the subscales vanish on the element boundaries. This approximation is not sufficient to obtain a numerical method because the space of subscales is still infinite dimensional (the "broken" space $\cup_K H_0^1\left(K\right)$, for example) and therefore the subscale problem (20)-(22) is as difficult as the original continuous problem. To deal with the subscales problem we will adopt a simple approximation that can be found, for example, in (Codina, 2002) and references therein.

The differential equations (20)-(22) over each element domain Ω_e can be written in vectorial form as

$$\widetilde{P}\left(\boldsymbol{M}\frac{\partial\widetilde{\boldsymbol{U}}}{\partial t}+\mathcal{L}\widetilde{\boldsymbol{U}}\right)=\widetilde{P}\left(\boldsymbol{R}\right)\quad\text{in}\quad\Omega_e$$

where $\widetilde{\boldsymbol{U}}\equiv\left[\widetilde{\boldsymbol{u}},\widetilde{p},\widetilde{T}\right]$, $\mathcal{L}$ is a differential vector operator, $\boldsymbol{M}$ is the $(d+2)\times(d+2)$ diagonal matrix $\boldsymbol{M}=\text{diag}\left(\rho^h\boldsymbol{I}_d,0,\rho c_p\right)$, where $\boldsymbol{I}_d$ is the $d\times d$ identity matrix, and $\boldsymbol{R}\equiv[\boldsymbol{R}_m,R_c,R_e]$. In the present work we will consider the space of subscales as that of the residuals, that is we will consider $\widetilde{P}=\boldsymbol{I}$ (the identity) when applied to the finite element residuals. Another possibility, advocated in (Codina, 2002), consists in taking $\widetilde{P}$ as the projection onto the space orthogonal to the finite element space. This leads to better accuracy and a clear identification of the energy transfer mechanisms between the finite element scales and the subscales (Principe et al., 2010).

We consider the algebraic approximation $\mathcal{L}\approx\boldsymbol{\tau}^{-1}$ in each Ω_e, where $\boldsymbol{\tau}$ is an $(d+2)\times(d+2)$ diagonal matrix. Taking $\boldsymbol{\tau}=\text{diag}(\tau_m\boldsymbol{I}_d,\tau_c,\tau_e)$ the approximation to the subscales equations (20)-(22) within each element of the finite element partition reads

$$\frac{1}{\tau_c}\widetilde{p} = R_c \tag{26}$$

$$\rho^h\frac{\partial\widetilde{\boldsymbol{u}}}{\partial t}+\frac{1}{\tau_m}\widetilde{\boldsymbol{u}} = \boldsymbol{R}_m \tag{27}$$

$$\rho^h c_p\frac{\partial\widetilde{T}}{\partial t}+\frac{1}{\tau_e}\widetilde{T} = R_e \tag{28}$$

In this way, the subscales are approximated at every finite element in a closed form in terms of the finite element residuals. The stabilization parameters are computed as

$$\tau_c = \frac{h^2}{c_1\rho^h\tau_m}=\frac{\mu}{\rho^h}+\frac{c_2}{c_1}|\boldsymbol{u}_h+\widetilde{\boldsymbol{u}}|h \tag{29}$$

$$\tau_m = \left(c_1\frac{\mu}{h^2}+c_2\frac{\rho^h|\boldsymbol{u}_h+\widetilde{\boldsymbol{u}}|}{h}\right)^{-1} \tag{30}$$

$$\tau_e = \left(c_1\frac{k}{h^2}+c_2\frac{\rho^h c_p|\boldsymbol{u}_h+\widetilde{\boldsymbol{u}}|}{h}\right)^{-1} \tag{31}$$

where h is the element size and c_1 and c_2 are algorithmic constants (we have adopted $c_1=4$ and $c_2=2$ in the numerical experiments using linear elements).

It is important to remark that (27) and (28) are nonlinear equations as the velocity subscale contributes to the advection velocity in momentum and energy residuals and also in the stabilization parameters τ_m, τ_e. The temperature subscale contributes through ρ^h to the residuals and to coefficients τ_m,τ_e.

When the time derivative of the subscales is neglected, we will call them *quasi-static,* whereas otherwise we will call them *dynamic.* The semi-discrete in space formulation is now complete, but contrarily to what happens with linear quasi-static subscales it is not possible to obtain a closed-form expression for dynamic subscales and insert them into (15)-(17) to obtain a problem for the finite element unknowns only. Before discretizing in time we cannot go any further than saying that the problem consists in solving (15)-(17) together with (26)-(28). This final semidiscrete system of equations is highly nonlinear, even more when nonlinear subscales are considered. However, it is not the purpose of the present work to discuss how to linearize it.

The linearization scheme introduced in (Principe and Codina, 2007) is applied to Eqs. (15)-(17) and the nonlinear terms in (27) and (28) are treated by fixed-point-like strategies, although other possibilities can be devised.

4 TIME DISCRETIZATION

Any time integration scheme can now be applied to discretize in time both equations (15) - (17), together with Eqs.(27) - (26). To be specific, we will consider the trapezoidal rule. Let Δt be the time step size of a uniform partition of the time interval $[0,T]$, $0 = t^0 < t^1 < ... < t^N = T$. Functions approximated at time t^n will be identified with the superscript n. For a generic function f, we will use the notation $\delta f^n := f^{n+1} - f^n$, $\delta_t f^n = \delta f^n/\Delta t$, $f^{n+\theta} = \theta f^{n+1} + (1-\theta) f^n, 0 \leq \theta \leq 1$.

The time discretization of the finite element equations (15)-(17) is standard and therefore we restrict our attention to the subgrid scales equations. As it is discussed in (Codina et al., 2007) the time integration for the subscales could be less accurate than for the finite element equations without affecting the accuracy of the scheme. Discretization in time of the subscales equations(26)-(28) yields to

$$\widetilde{p}^{n+\theta} = \tau_c^{n+\theta} R_c^{n+\theta} \tag{32}$$

$$\widetilde{\boldsymbol{u}}^{n+\theta} = \left(\frac{\rho^h}{\theta \Delta t} + \frac{1}{\tau_m^{n+\theta}} \right)^{-1} \left(\boldsymbol{R}_m^{n+\theta} + \frac{\rho^h \widetilde{\boldsymbol{u}}^n}{\theta \Delta t} \right) \tag{33}$$

$$\widetilde{T}^{n+\theta} = \left(\frac{\rho^h c_p}{\theta \Delta t} + \frac{1}{\tau_e^{n+\theta}} \right)^{-1} \left(R_e^{n+\theta} + \frac{\rho^h c_p \widetilde{T}^n}{\theta \Delta t} \right) \tag{34}$$

From these expressions, we see that the residual of the momentum and energy equations are multiplied respectively by

$$\tau_{tm} = \left(\frac{\rho^h}{\theta \Delta t} + \frac{1}{\tau_m^{n+\theta}} \right)^{-1} \tag{35}$$

$$\tau_{te} = \left(\frac{\rho^h c_p}{\theta \Delta t} + \frac{1}{\tau_e^{n+\theta}} \right)^{-1} \tag{36}$$

These can be considered the stabilization parameters for the transient Low Mach equations. Expressions with asymptotic behavior similar to coefficients τ_{tm}, τ_{te} in terms of $h, \mu, |\boldsymbol{u}_h + \widetilde{\boldsymbol{u}}|$, and Δt can be often found in the literature (see e.g. (Gravemeier and Wall, 2010b)). It is important to note that if the stabilization parameter depends on Δt and subscales are not considered time dependent, *the steady-state solution will depend on the time step size*. This does not happen if expressions (33) and (34) are used. It can be checked that, when steady state is reached the usual expressions employed for stationary problems are recovered, namely $\widetilde{\boldsymbol{u}} = \tau_m \widetilde{P}(\boldsymbol{R}_m)$, and $\widetilde{T} = \tau_e \widetilde{P}(R_e)$. From the point of view of the algebraic solver, to use $\boldsymbol{\tau}_{tm}, \boldsymbol{\tau}_{te}$ instead of $\boldsymbol{\tau}_m, \boldsymbol{\tau}_e$ is crucial for the conditioning of the system matrix.

5 GLOBAL CONSERVATION PROPERTIES

The aim of this section is to obtain global conservation statements similar to those holding for the continuous problem (1)-(3) but not necessary for the discrete one. To do that it is necessary to consider the finite element spaces without Dirichlet boundary conditions and an augmented problem that also contains the tractions at the Dirichlet boundaries as unknowns (Hughes et al.,

2000). This permits to take constant test functions (see below) and to arrive to conservation statements in terms of the tractions and flows at the boundaries.

5.1 Mass conservation

Taking the test function $q_h = 1$ in the mass equation (15) global mass conservation follows immediately

$$\int_\Omega \frac{\partial \rho^h}{\partial t} d\Omega = -\int_{\partial\Omega} \boldsymbol{n}\cdot\rho^h \boldsymbol{u}_h d\Gamma \tag{37}$$

5.2 Momentum Conservation

Taking the tests function $\boldsymbol{v}_h = (1,0,0)\,;(0,1,0)$ and $(0,0,1)$ in (the augmented problem corresponding to) the finite element momentum equation (16), multiplying them respectively by unit vectors pointing in the coordinate directions and adding them, we get

$$\begin{aligned}\int_\Omega \rho^h \frac{\partial}{\partial t}\left(\boldsymbol{u}_h + \widetilde{\boldsymbol{u}}\right) d\Omega + \int_\Omega \rho^h \left(\boldsymbol{u}_h + \widetilde{\boldsymbol{u}}\right)\cdot\boldsymbol{\nabla}\boldsymbol{u}_h d\Omega \\ + \int_\Omega \widetilde{\boldsymbol{u}}\frac{\partial \rho^h}{\partial t} d\Omega = \int_\Omega \rho^h \boldsymbol{g} d\Omega + \int_{\partial\Omega} \boldsymbol{t}_n d\Gamma\end{aligned} \tag{38}$$

When using equal interpolation spaces for the velocity components and pressure equations, we can take the test function equal to velocity components $q_h = v_{h,i}$ in the discrete mass equation (15). Therefore, we get the relation

$$\int_\Omega \rho^h \left(\boldsymbol{u}_h + \widetilde{\boldsymbol{u}}\right)\cdot\boldsymbol{\nabla}\boldsymbol{u}_h d\Omega = \int_\Omega \left(\frac{\partial \rho^h}{\partial t}\right)\boldsymbol{u}_h d\Omega + \int_{\partial\Omega} \left(\boldsymbol{n}\cdot\boldsymbol{u}_h\right)\rho^h \boldsymbol{u}_h d\Gamma$$

Replacing in (38) we arrive to

$$\begin{aligned}\int_\Omega \rho^h \frac{\partial}{\partial t}\left(\boldsymbol{u}_h + \widetilde{\boldsymbol{u}}\right) + \int_\Omega \left(\boldsymbol{u}_h + \widetilde{\boldsymbol{u}}\right)\frac{\partial \rho^h}{\partial t} d\Omega \\ = \int_\Omega \rho^h \boldsymbol{g} d\Omega + \int_{\partial\Omega} \left(\boldsymbol{t}_n - \left(\boldsymbol{n}\cdot\boldsymbol{u}_h\right)\rho^h \boldsymbol{u}_h\right) d\Gamma\end{aligned}$$

If momentum is defined as $\boldsymbol{p} = \rho^h \boldsymbol{u}_h + \rho^h \widetilde{\boldsymbol{u}}$, with the contributions due to the finite element and the subscales components, we get the following conservation equation

$$\int_\Omega \frac{\partial \boldsymbol{p}}{\partial t} d\Omega = \int_\Omega \rho^h \boldsymbol{g} d\Omega + \int_{\partial\Omega} \boldsymbol{t}_n - \left(\boldsymbol{n}\cdot\boldsymbol{u}_h\right)\rho^h \boldsymbol{u}_h d\Gamma \tag{39}$$

This equality indicates that the change of the total momentum over the system is equal to the total force over the system plus the traction and momentum fluxes over the boundary $\partial\Omega$. Note that Eq.(39) holds independently of the subscale approximation.

5.3 Energy conservation

Taking the test function $w_h = 1$ in (the augmented problem corresponding to) the finite element energy equation (17) we get

$$\int_\Omega \left(\rho^h c_p \frac{\partial}{\partial t}\left(T_h + \widetilde{T}\right) + \rho^h c_p \left(\boldsymbol{u}_h + \widetilde{\boldsymbol{u}}\right)\cdot\nabla T_h + \widetilde{T} c_p \frac{\partial \rho^h}{\partial t}\right) d\Omega$$
$$= \int_\Omega \left(Q + \alpha \left(T_h + \widetilde{T}\right) \frac{dp^{th}}{dt}\right) d\Omega + \int_{\partial\Omega} q_n d\Gamma \tag{40}$$

When using equal interpolation spaces for the temperature and pressure equations ($W_h = Q_h$), we can take $q_h = T_h$ in the discrete mass equation (15) to obtain

$$\int_\Omega \rho^h \left(\boldsymbol{u}_h + \widetilde{\boldsymbol{u}}\right)\cdot\boldsymbol{\nabla} T_h d\Omega = \int_\Omega \left(\frac{\partial \rho^h}{\partial t}\right) T_h d\Omega + \int_{\partial\Omega} \rho^h \boldsymbol{n}\cdot\boldsymbol{u}_h T_h d\Gamma$$

Replacing this equality in (40) we get the relation

$$\int_\Omega c_p \frac{\partial}{\partial t}\left(\rho^h \left(T_h + \widetilde{T}\right)\right) d\Omega = \int_\Omega \left(Q + \alpha \left(T_h + \widetilde{T}\right) \frac{dp^{th}}{dt}\right) d\Omega + \int_{\partial\Omega} \left(q_n - \boldsymbol{n}\cdot\boldsymbol{u}_h \rho^h c_p T_h\right) d\Gamma \tag{41}$$

which is the discrete counterpart of energy conservation equation (3) integrated over domain Ω.

In the case of **ideal gases** (taking $p^{th} = \rho^h R\left(T_h + \widetilde{T}\right)$ with $R = \frac{\gamma-1}{\gamma} c_p$ and $\alpha = 1/\left(T_h + \widetilde{T}\right)$) equation (41) gets written as

$$\frac{|\Omega|}{\gamma - 1}\frac{dp^{th}}{dt} + \frac{\gamma p^{th}}{\gamma - 1}\int_{\partial\Omega} \boldsymbol{n}\cdot\boldsymbol{u}_h d\Gamma = \int_\Omega Q d\Omega + \int_{\partial\Omega} q_n d\Gamma \tag{42}$$

which is the discrete version of equation (8), implying global energy conservation. For ideal gases the specific internal energy is $e = c_p T/\gamma = \frac{1}{\gamma-1} p^{th}/\rho$. So, for the low Mach approximation internal energy per unit volume ρe is uniform and directly proportional to thermodynamic pressure p^{th}. According to that, we define at the discrete level, the discrete internal energy per unit volume as $\rho^h e^h = \frac{1}{\gamma-1} p^{th} = \rho^h c_p \left(T_h + \widetilde{T}\right)/\gamma$. Replacing this definition in Eq. (42), we arrive to the first law for open systems in terms of the internal energy

$$\int_\Omega \frac{\partial\left(\rho^h e_h\right)}{\partial t} d\Omega = \int_\Omega Q d\Omega + \int_{\partial\Omega} \boldsymbol{n}\cdot\left(k\nabla T_h - \boldsymbol{u}_h \rho^h e^h - \boldsymbol{u}_h p^{th}\right) d\Gamma \tag{43}$$

that indicates that the change of internal energy of the system is equal to the heat power added to the system plus the work done over the system ($W = -\int_{\partial\Omega} \boldsymbol{n}\cdot\boldsymbol{u}_h p^{th} = -p^{th}\int_\Omega \nabla\cdot\boldsymbol{u}_h d\Omega$) plus the boundary fluxes of heat and internal energy $\boldsymbol{n}\cdot k\nabla T_h$ and $\boldsymbol{n}\cdot\boldsymbol{u}_h\rho^h e^h$. It has been proved recently in (Codina et al., 2010) that for the Boussinesq approximation global conservation of energy is obtained when nonlinear and orthogonal subscales are used.

6 NUMERICAL EXAMPLES

In this section we present two examples already considered in the literature. The first is an example of the behavior of the formulation for the stationary equations, whereas the other is a transient compressible flow at low speed. In both examples we consider an ideal gas with constant values of $R = 287.0 \frac{\text{J}}{\text{Kg K}}$ and $c_p = 1004.5 \frac{\text{J}}{\text{Kg K}}$. The formulation presented in this paper will be compared to the algebraic subgrid scale (ASGS) method, as presented in (Principe and Codina, 2007), which is reduced to the GLS method (Heuveline, 2003) when linear elements are used. Bilinear interpolated elements Q_1 are used in both examples for velocity, pressure and temperature equations.

6.1 Natural convection in a cavity

This flow example was also considered in e.g., (Heuveline, 2003; Principe and Codina, 2007; Gravemeier and Wall, 2010b). The problem domain is $\Omega = [0, L] \times [0, L]$ with $L = 1$ m. Adiabatic boundary conditions are prescribed for upper and lower walls $(q_n = k\boldsymbol{n} \cdot \nabla T_h = 0)$. The left wall is maintained at a fixed temperature T_H and the right wall at temperature T_C. The initial thermodynamic pressure and temperatures are $p_0^{th} = 101325$Pa, $T_0 = 600$K, yielding an initial uniform density of $\rho_0 = 0.58841$Kg/m^3. In contrast to the Boussinesq approximation, in low Mach approximation the stationary solution depends on the initial thermodynamic pressure p_0^{th}. The dimensionless Prandtl and Rayleigh numbers are fixed to $\mathrm{Pr} = \frac{c_p \mu}{k} = 0.71$, $\mathrm{Ra} = 2\frac{||\boldsymbol{g}||\rho_0^2}{\mu^2}\varepsilon = 10^6$, where $\varepsilon = \frac{T_H - T_C}{T_H + T_C} = 0.6$ .The viscosity is $\mu = 10^{-3}\frac{\mathrm{Kg}}{\mathrm{m\,s}}$. Boundary left and right wall temperatures are $T_H = 960$K and $T_C = 240$K satisfying the relation $(T_H + T_C)/2 = T_0$. Zero Dirichlet boundary conditions for the velocity are assumed on all boundaries.

The results were obtained using a mesh of 20×20 uniform elements. The reference solution was obtained using a grid of 180×180 uniform elements with the ASGS method. The streamlines and temperature solutions are depicted in Fig. 1.

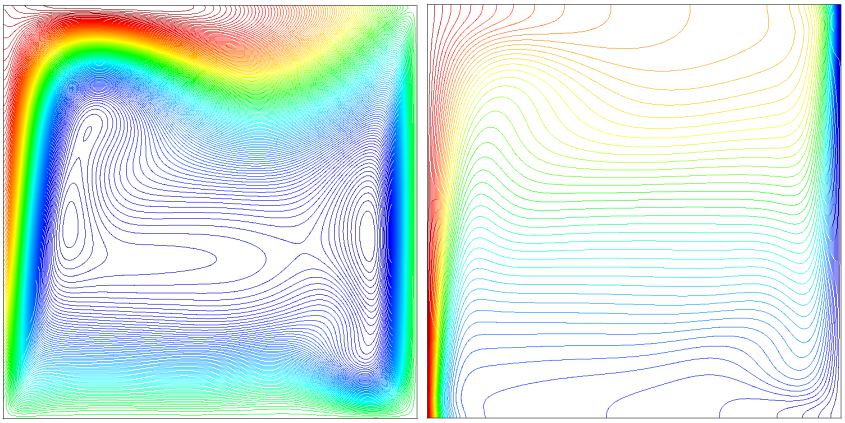

Figure 1: Streamlines and Temperature solutions

Cuts of velocity and temperature solutions for different stabilization methods are depicted in Fig. 2 using a mesh of 20×20 elements. The compared stabilization methods are:

- The method in the present paper containing full nonlinear subscales, labeled as "FullSGS" in Fig. 2.
- The method presented in this paper, but neglecting temperature subscale in the state equation, that is $\rho^h = \frac{p^{th}}{RT_h}$, labeled as "SemiSGS" in Fig. 2.
- The method presented in this paper, but using a linear approximation to the subscales Eqs. (26)- (28), that is, taking τ_m, τ_c, τ_e and $\boldsymbol{R}_m, R_c, R_e$ independent of the velocity and temperature subscales $\widetilde{\boldsymbol{u}}$, $\widetilde{T}$. In all cases $|\boldsymbol{u}_h + \widetilde{\boldsymbol{u}}|$ is replaced by $|\boldsymbol{u}_h|$ as it is usually done, for example in (Gravemeier and Wall, 2010b) or (Bazilevs et al., 2007). As in the previous case the temperature subscale is neglected in the state equation. This method is labeled as "LinSGS" in Fig. 2.
- The ASGS method, a linear stabilization method as described in (Principe and Codina, 2007).

- The reference solution, labeled as "Ref" in Fig. 2.

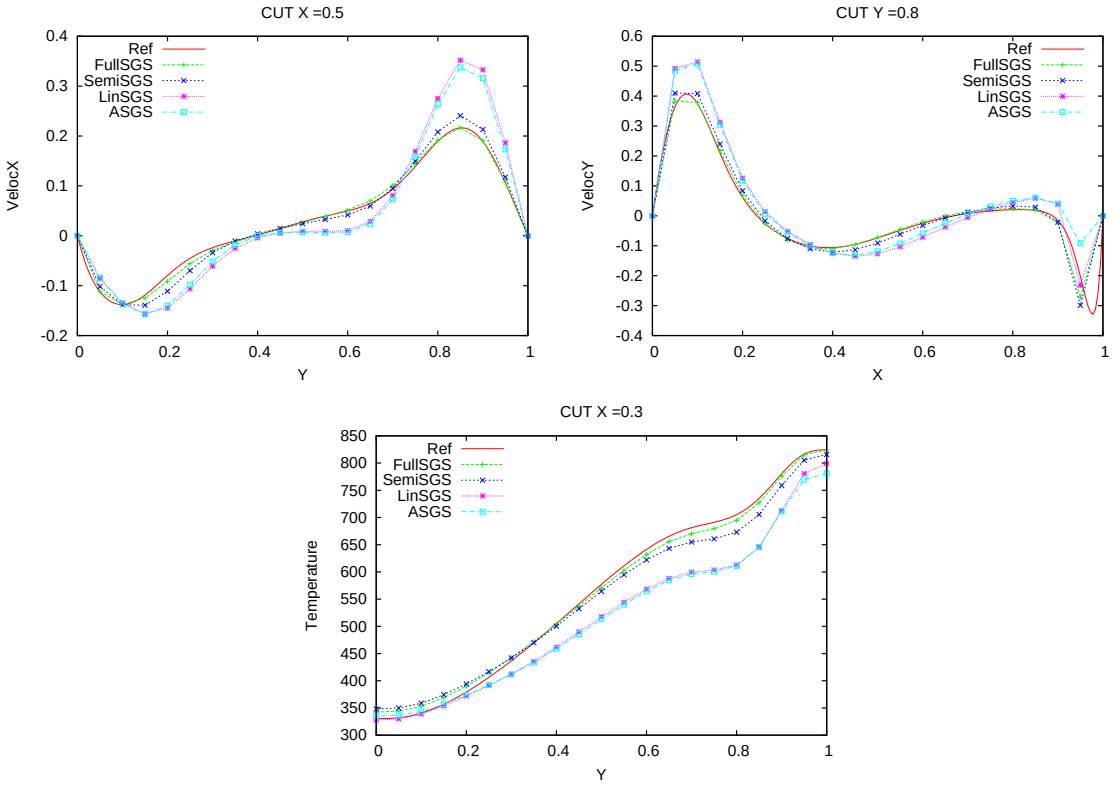

Figure 2: Cuts of the solution for different stabilization methods against a reference solution

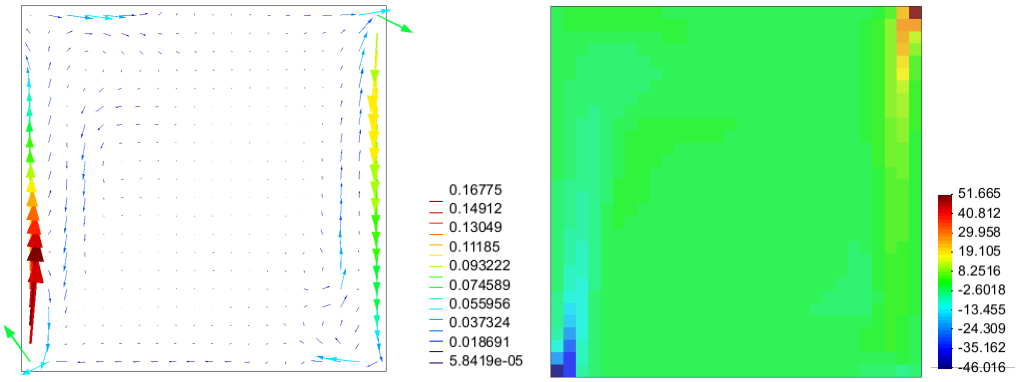

Figure 3: Velocity and Temperature subscales

The higher accuracy of the solution obtained when subscales are kept in all the nonlinear terms, both in the the finite element equations and in the subscales equations, can be clearly observed in Fig. 2. When the temperature subscale is neglected in the state equation the solution is less accurate. Finally when a linear approximation to the subscales Eqs.(26)- (28 is considered, even less accurate solutions are obtained.

Velocity subscales and temperature subscale modulus are depicted in Fig.3. As expected the subscales are bigger near the boundaries, where velocity and temperature gradients are large.

6.2 Transient injection flow at low Mach regime

This flow example was recently proposed in (Beccantini et al., 2008), and also considered by (Gravemeier and Wall, 2010b). The problem domain is $\Omega = [-L/2, L/2] \times [0, H]$, where $L = 3$m and $H = 7$m. The initial values are $T_0 = 300$K and $p_0^{th} = 10^5$Pa resulting in an initial density of $1.161 \frac{\text{Kg}}{\text{m}^3}$. Furthermore $\mu = 0.005 \frac{\text{Kg}}{\text{m s}}$ and $\text{Pr} = 0.71$. Zero Dirichlet boundary conditions for the velocity are assumed on all boundaries, except for a small hole in the bottom wall at $[-l/2, l/2]$ where $l = 0.2$m. Through this hole fluid is injected subject to a parabolic inflow profile $\boldsymbol{u}_d = (0, 2.5830\,(1.0 - 100x^2))$m/s. The temperature of the injected fluid is $T_D = 600$K. Aside from this, adiabatic boundary conditions are prescribed in all boundaries. We consider a gravity $\boldsymbol{g} = (0, -9.81)$m/s^2.

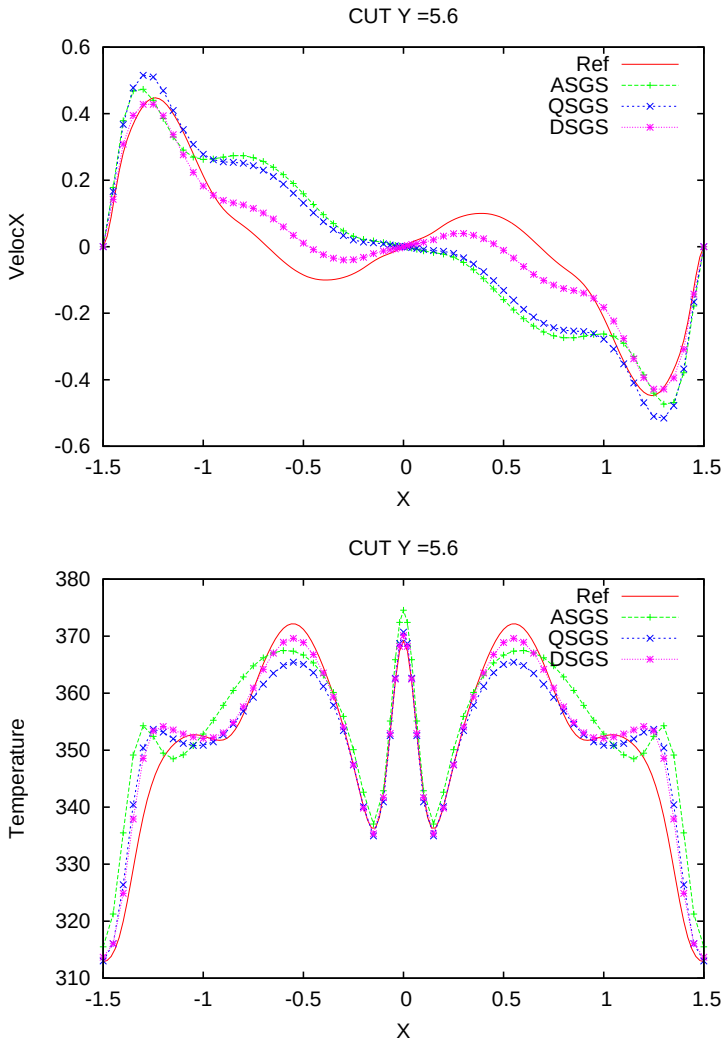

Figure 4: Cuts of the solution at $y = 5.6$m when $t = 0.6$s for different stabilization methods against a reference solution.

The domain is discretized with 60×60 elements, and the time step size is chosen to be $\Delta t = 0.06$s. The computation is advanced until $\text{t}_{\text{end}} = 6.0$s. The second order time integration scheme BDF2 was used.

The results obtained with our stabilization method using dynamic (DSS) and quasistatic

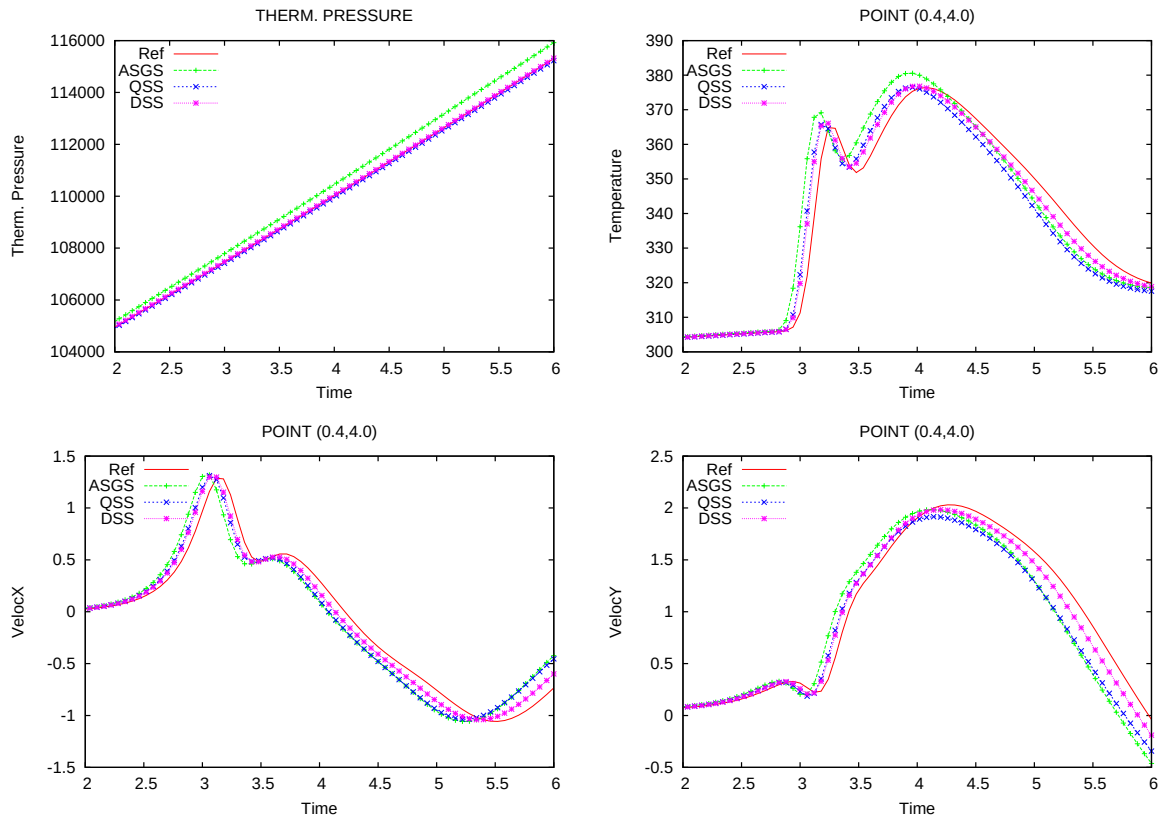

Figure 5: Point evolution of the unknowns using different stabilization methods; QSS (DSS) indicates nonlinear and quasistatic (dynamic) subscales.

(QSS) subscales are compared to those obtained using the ASGS method and a reference solution obtained using a mesh of 180×180 uniform elements and the ASGS method. Cuts of temperature and x-velocity fields at $y = 5.6$m and $x = 0.2$m when $t = 6$ s are depicted in Fig. 4. As in the previous example, a gain in accuracy is observed when the method of dynamic and non nonlinear subscales is used. Time evolutions of thermodynamic pressure, velocities and temperature at point $(0.4, 4.0)$ m are compared in Fig. 5. This figure shows a higher temporal accuracy of the scheme when nonlinear subscales are used and even higher when transient subscales are considered.

It is important to remark that the use of nonlinear subscales results in an increase in the cost of the solution of the nonlinear problem (in terms of number of iterations). This is the expected price to be paid for the gain in accuracy. However we should also point out that when using transient subscales this cost increase is smaller than when using static subscales even if the gain in accuracy is bigger.

7 CONCLUSIONS

In this article a new stabilized finite element approximation of the low Mach number equations has been developed based on scale separation. The main ingredients of the formulation, developed are

- to consider time dependent subscales
- to keep the subscale components in all the nonlinear terms

The effect of considering time dependent subscales is well known (Codina et al., 2007) and our experience with the low Mach number equations confirms the properties known for incompressible flow. Apart from theoretical aspects (dependence of the stabilization parameters with the time step size, time step independent steady state solutions, convergence proofs for any time step) the use of time dependent subscales results in a better conditioning of the system matrix.

In turn, the effect of considering the splitting of the unknowns in all the terms (including the state equation) leads to a more accurate solution and provides global mass, momentum and energy conservation when using equal interpolation spaces for the velocity, pressure and temperature equations. The formulation contains cross- and Reynolds- stress terms, and presents an open door to turbulence modelling. The present method remains unchanged irrespective of whether laminar, transitional and turbulent situations are present. Nevertheless, the adequacy of the present method for turbulent flows situations remains to be investigated. We intend to do this in our future work.

REFERENCES

Bazilevs Y., V.M.Calo, Cottrell J., Hughes T., and A. Reali G.S. Variational multiscale residual-based turbulence modeling for large eddy simulation of incompressible flows. *Computer Methods in Applied Mechanics and Engineering*, 197:173–201, 2007.

Beccantini A., Studer E., Gounand S., Magnaud J., and Kloczko T. Numerical simulations of a transient injection flow at low mach number regime. *International Journal for Numerical Methods in Engineering*, 76:662–696, 2008.

Boris J.P., Grinstein F.F., Oran E.S., and Kolbe R.L. New insights into large eddy simulation. *Fluid Dynamics Research*, 10(4-6):199, 1992.

Codina R. Comparison of some finite element methods for solving the diffusion-convection-reaction equations. *Computer Methods in Applied Mechanics and Engineering*, 156:185–210, 1998.

Codina R. A stabilized finite element method for generalized stationary incompressible flows. *Computer Methods in Applied Mechanics and Engineering*, 190(20–21):2681–706, 2001.

Codina R. Stabilized finite element approximation of transient incompressible flows using orthogonal subscales. *Computer Methods in Applied Mechanics and Engineering*, 191:4295–4321, 2002.

Codina R., Principe J., and Avila M. Finite element approximation of turbulent thermally coupled incompressible flows with numerical sub-grid scale modelling. *International Journal of Numerical Methods for Heat and Fluid Flow*, 20(5):492–516, 2010.

Codina R., Principe J., O.Guasch, and S.Badia. Time dependent subscales in the stabilized finite element approximation of incompressible flow problems. *Computer Methods in Applied Mechanics and Engineering*, 196:2413–2430, 2007.

Gravemeier V. and Wall W. An algebraic variational multiscale-multigrid method for large-eddy simulation of turbulent variable-density flow at low mach number. *Journal of Computational Physics*, 229:6047–6070, 2010a.

Gravemeier V. and Wall W. Residual-based variational multiscale methods for laminar transitional and turbulent variable-density flow at low mach number. *International Journal for Numerical Methods in Fluids*, n/a, 2010b. doi:10.1002/fld.2242.

Guasch O. and Codina R. A heuristic argument for the sole use of numerical stabilization with no physical les modelling in the simulation of incompressible turbulent flows. *Submitted*, 2010.

Heuveline V. On higher- order mixed fem for low mach number flows: Applications to a natural convection benchmark problem. *International Journal for Numerical Methods in Fluids*, 41:1339–1356, 2003.

Hughes T., Emgel G., Mazzei L., and Larson M. The continuous galerkin method is locally conservative. *Journal of Computational Physics*, 163:467–488, 2000.

Hughes T., Scovazzi G., and Franca L. Multiscale and stabilized methods. In T.H. E. Stein R. de Borst, editor, *Enciclopedia of Computational Mechanics*. Willey: Chichester, 2004.

Hughes T.J.R., Feijóo G.R., Mazzei L., and Quincy J. The variational multiscale method– a paradigm for computational mechanics. *Computer Methods in Applied Mechanics and Engineering*, 166:3–24, 1998.

Hughes T.J.R., Franca L., and Balestra M. A new finite element formulation for computational fluid dynamics: V. circumventing the babuska-brezzi condition: a stable petrov galerkin foormulation of the stokes problem accomodating equal order interpolations. *Computer Methods in Applied Mechanics and Engineering*, 59(1):85–99, 1986.

Lions P. *Mathematical Topics in Fluid Dynamics, Volume 2. Compressible Models*. Oxford University Press, 1996.

Majda A. and Sethian J. The derivation and numerical solution of the equations for zero mach number combustion. *Combustion Science and Technology*, 42:185–205, 1985.

Principe J. and Codina R. A stabilized finite element approximation of low speed thermally coupled flows. *International Journal of Numerical Methods for Heat and Fluid Flow*, 18:835–867, 2007.

Principe J. and Codina R. Mathematical models for thermally coupled low speed flows. *Advances in Theoretical and Applied Mechanics*, 2:93–112, 2009.

Principe J., Codina R., and Henke. F. The dissipative structure of variational multiscale methods for incompressible flows. *Computer Methods in Applied Mechanics and Engineering*, 199:791–801, 2010.